Composite Structures 251 (2020) 112591

Contents lists available at ScienceDirect

Composite Structures

journal homepage: www.elsevier.com/locate/compstruct

Enhanced vibration and damping characteristics of novel corrugated sandwich panels with polyurea-metal laminate face sheets

Xin Wang [a,c], Xue Li [b,c], Run-Pei Yu [a,c], Jian-Wei Ren [b,c], Qian-Cheng Zhang [a,d,*], Zhen-Yu Zhao [b,c], Chang-Ye Ni [b,c], Bin Han [e], Tian Jian Lu [b,c,*]

[a] State Key Laboratory for Strength and Vibration of Mechanical Structures, Xi'an Jiaotong University, Xi'an 710049, PR China
[b] State Key Laboratory of Mechanics and Control of Mechanical Structures, Nanjing University of Aeronautics and Astronautics, Nanjing 210016, PR China
[c] Nanjing Center for Multifunctional Lightweight Materials and Structures (MLMS), Nanjing University of Aeronautics and Astronautics, Nanjing 210016, PR China
[d] Key Laboratory of Intense Dynamic Loading and Effect, Northwest Institute of Nuclear Technology, Xi'an 710024, PR China
[e] School of Mechanical Engineering, Xi'an Jiaotong University, Xi'an 710049, PR China

ARTICLE INFO

Keywords:
Vibration damping
Sandwich panels
Viscoelastic polyurea
Laser welding

ABSTRACT

All-metallic sandwich panels with lattice truss cores are typically ultralight, stiff and strong, yet poor in passive vibration damping. Novel laser-welded corrugated-core (LASCOR) sandwich panels with polyurea-metal laminates (PML) as face sheets were proposed and fabricated, and their vibration and damping characteristics were systematically investigated, both experimentally and numerically. Frequency/time response curves, natural frequencies, vibration mode shapes and damping loss factors were measured and compared with LASCOR sandwich panels without embedded polyurea layers. A combined finite element-modal strain energy (FE-MSE) method was proposed to predict the vibration damping performance and explore the underlying enhancement mechanisms, with the frequency-dependent damping behaviors of polyurea considered. Good agreement was achieved between numerical simulations and experimental measurements. The PML face sheets enabled remarkable damping enhancement, due mainly to viscoelastic energy dissipation of the polyurea layers. The capacity of the sandwich panel in passive vibration suppression could be further improved by tailoring the polyurea layer thickness and the distribution of polyurea layers.

1. Introduction

For ultralight, all-metallic sandwich constructions, a variety of core topological configurations including two-dimensional (2D) and three-dimensional (3D) lattices have been exploited [1,2]. Correspondingly, extensive studies have been carried out to characterize their mechanical properties [3–9], such as compression, shearing, bending and blast resistance, as well as vibration damping. With pressing need for vibration and sound suppression, damping has attracted increasing attention. For instance, damping plays a key role in the prevention of early structural damage caused by resonant vibration in engineering applications (*e.g.*, ship hulls, automotive bodies, and pulse detonation engines). Nevertheless, limited by the typically low loss factor (magnitude on the order of $10^{-5} \sim 10^{-3}$) of the parent material [10,11], all-metallic sandwich constructions exhibit obvious shortcomings in the passive control of undesirable vibration and noise. Thus, to deal with the complex service environment, there is a long-standing need to improve the vibration and damping characteristics of all-metallic sandwich structures by making appropriate modifications to their face sheets and cores.

Recently, the method of viscoelastic layer treatment has been envisioned as an effective way to suppress the excessive vibration of metallic and composite structures. Specifically, one or more viscoelastic layers are combined with a base material layer to construct a laminate with excellent combination of damping loss factor and structural stiffness. Thus far, the two most commonly-adopted laminate configurations are the base/viscoelastic/base laminates with constrained layer damping (CLD) [12] and the viscoelastic/base laminates with free layer damping (FLD) [13]. It has been demonstrated that the CLD laminates exhibited a greater damping capacity due to transverse shear deformation of the viscoelastic layer, while the FLD laminates almost relied on both in-plane extension and compression deformation to dissipate the vibration energy [14]. Nonetheless, optimizing the distribution of viscoelastic material in a FLD laminate could lead to enhanced

* Corresponding authors at: State Key Laboratory for Strength and Vibration of Mechanical Structures, Xi'an Jiaotong University, Xi'an 710049, PR China (Q.C. Zhang). State Key Laboratory of Mechanics and Control of Mechanical Structures, Nanjing University of Aeronautics and Astronautics, Nanjing 210016, PR China (T.J. Lu).
E-mail addresses: zqc111999@xjtu.edu.cn (Q.-C. Zhang), tjlu@nuaa.edu.cn (T.J. Lu).

https://doi.org/10.1016/j.compstruct.2020.112591
Received 5 March 2020; Revised 20 May 2020; Accepted 3 June 2020
Available online 23 June 2020

damping performance [15]. More recently, the CLD treatment was utilized to construct the face sheets of an all-composite lattice-core sandwich structure [16–18]. By sandwiching the fiber-reinforced composite face sheet with thin viscoelastic layers, the damping and stiffness efficiency of the sandwich structure was dramatically improved. The modal damping properties as well as the underlying mechanisms of novel composite auxetic double-arrow corrugated sandwich panels were also investigated [19,20]. In addition, the effects of temperature rise on modal characteristics of composite honeycomb-core sandwich panels were identified numerically and experimentally [21]. At present, the vibration damping characteristics of ultralight, all-metallic sandwich panels having 2D/3D lattice cores remain elusive. The current study aims therefore to explore how their vibration damping properties could be significantly enhanced by introducing viscoelastic layer treatment to the face sheets. To this end, selection of a viscoelastic material with a sufficiently high damping loss factor becomes important.

Currently, there is bourgeoning research interest in an eco-friendly polymeric material called polyurea elastomer, which exhibits versatile features, including anti-impact, anti-corrosion, waterproof, and damping capacity. Formed from the reaction of isocyanate and amine, the polyurea possesses hard domains dispersed randomly within soft domains, exhibiting a heterogeneous landscape with nano-segregated microstructure [22]. As a type of viscoelastic material, the polyurea exhibits strong strain rate sensitivity and damping loss behaviors [23,24]. Thus, coating metal or fiber-reinforced composite plates with polyurea layers has become an effective strategy to significantly improve the survivability of such structures under high intensity impulsive loadings, especially for those encountered in blast/impact events [25–27]. It is natural therefore that existing researches of polyurea have mainly focused upon its anti-blast/impact potential, with little attention paid to its vibration attenuation capacity.

The current study proposed to coat the face sheets of an all-metallic corrugated-core sandwich panel with polyurea layers for enhanced passive vibration attenuation. A combined experimental and numerical approach was adopted to carry out the investigation. The paper was organized as follows. Section 2 presented details concerning the fabrication procedures of corrugated sandwich panels with polyurea-metal laminate face sheets. The theoretical basis underlying subsequent modal vibration tests with the fabricated sandwich panels was also briefly introduced. In Section 3, the method of coupled finite element-modal stain energy (FE-MSE) was introduced to predict the vibration and damping performance of such structures, with the frequency-dependent damping characteristics of polyurea accounted for. Section 4 provided a comprehensive experimental comparison of sandwich panels with and without polyurea coating, and then analyzed the physically mechanisms underlying the remarkable damping enhancement. Numerical predictions of the FE-MSE method were validated against experimental measurements and further employed to assess how the polyurea layer thickness and the distribution of polyurea layers affect vibration damping.

2. Experimental methodology

Four different types of laser-welded corrugated-core (LASCOR) sandwich panels with polyurea-metal laminate (PML) face sheets were fabricated and tested, as shown in Fig. 1. Two types of PML face sheet were employed: steel/polyurea/steel laminate (PML-A) and steel/polyurea laminate (PML-B). Detailed geometrical parameters of the test samples are sketched in Fig. 1 and listed in Table 1. Each sample consisted of 14 unit cells, with an approximate length of 390 mm and a width of 140 mm. Relative density of the corrugated core $\bar{\rho}$ can be expressed as:

$$\bar{\rho} = \frac{t_c(l_p + l_c)}{(l_p + l_c\cos\theta)(t_c + l_c\sin\theta)} \tag{1}$$

2.1. Fabrication process

The corrugated cores were fabricated first using the stamping process. For enhanced bonding between the corrugated core and the face sheets, a corrugation platform was reserved as shown in Fig. 1. To minimize the effect of likely joint loss during welding, the thickness t_c of the corrugation member was required to be larger than 0.2 mm to ensure node integrity. As shown in Fig. 2, the LASCOR panel without polyurea coating was made from 304 stainless steel via laser welding. With reference to Fig. 2a-b, a YAG laser generator was mounted on an industrial robot, which could push the laser spot over the welding components at a fixed welding velocity. The corrugated core and the face sheets were fixed together by a pair of fixtures and a pressure beam. A shielding gas pipe followed the motion of the laser spot, releasing helium gas to protect the welding joints. The advantages of using helium gas included: (i) avoiding the focusing lens from sputtering of molten metal droplets, (ii) eliminating the plasmas produced during the process of laser welding, and (iii) reducing the undesirable oxidization of the welding joints. In the current study, as sandwich components with different thickness were bonded in sequence, three welding conditions between steel plates having different thicknesses need to be considered: 0.5 mm − 0.5 mm, 0.5 mm − 1.0 mm, 1.0 mm − 0.5 mm. A series of preliminary experiments were carried out to obtain desirable welding parameters prior to laser welding, as listed in Table 2. The most concerned parameters of laser welding included power, welding speed, shielding gas flow, focal and point position, which affected directly bonding strength and toughness.

To evaluate the welding quality, standard tensile-shear tests of laser-welded lap joint specimens were conducted. For illustration, consider the welding condition (1.0 mm − 0.5 mm), i.e., between 1.0 mm thick and 0.5 mm thick steel plates. Marked by red circles in Fig. 3a, the onset of fracture occurred in the parent material instead of the lap joint, indicating that the bonding strength exceeded the ultimate tensile strength of the parent material. Besides, the front side (1.0 mm steel), the back side (0.5 mm steel), and the cross section of the welding joint were observed under optical microscope. The images shown in Fig. 3b–d suggested that the welding parameters adopted in this study yielded approximately complete penetration. An approximately inverted conical shape of fusion profile was formed between the face sheet and the corrugated core, and there was no obvious imperfection generated in the cross section (Fig. 3d). Similar conclusions held for the remaining welding conditions considered. The as-fabricated LASCOR sandwich panel without polyurea coating was displayed in Fig. 4a.

To fabricate LASCOR sandwich panels with PML face sheets, the polyurea material selected was obtained from the reaction of a polycarbodiimide-modified diphenylmethane diisocyanate and amine terminated polyether (Qtech-413, Qingdao Shamu Advanced Material Co., Ltd.). The stoichiometric ratio of 1:1 isocyanate to amine was used to ensure complete chemical reaction. Firstly, the two separate components were placed into a vacuum drying oven with 1 torr vacuum until most of the entrapped air bubbles were removed. Then, the mixture was mechanically stirred for 1–2 min with a rate of 1000 rmp (motor stirrer, JJ-1H). As-fabricated LASCOR sandwich panels were placed in the acrylic mold, covered using the release paper. The mixture was poured immediately on the outer surface of the face sheet(s), which flowed slowly until uniformly covering the face sheet(s). Four hours later, another 304 stainless steel plate was put on the surface of the chemical mixture in order to prepare a PML-A face sheet. Subsequently, all the sandwich panels were cured at room temperature for

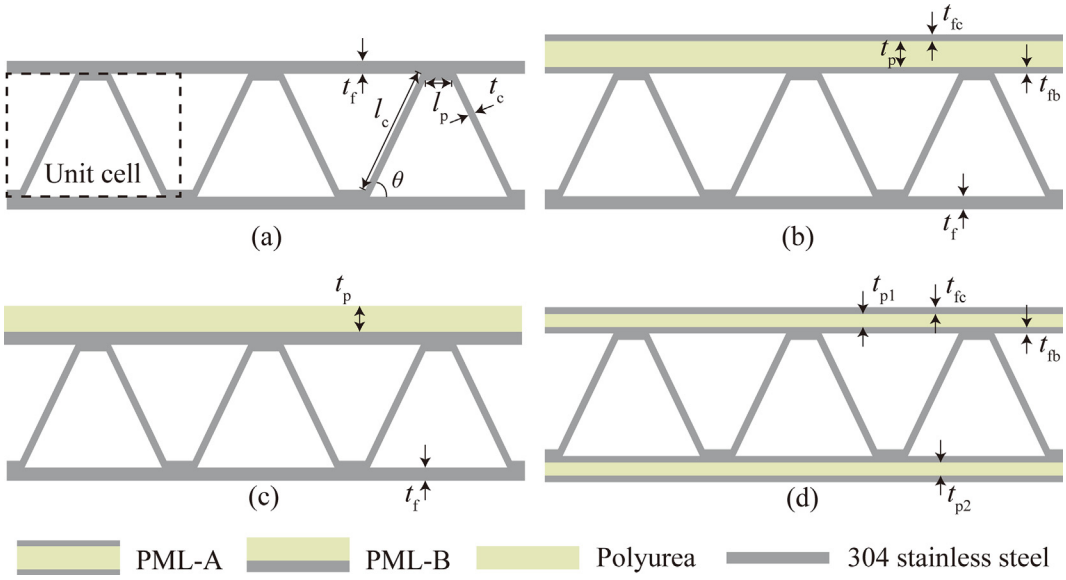

Fig. 1. Geometric illustration of corrugated sandwich panel (a) without polyurea coating, (b) with single PML-A face sheet, (c) with single PML-B face sheet, and (d) with double PML-A face sheets.

Table 1
Geometric parameters of as-fabricated corrugated sandwich panels (unit: mm).

Specimen	Face sheet configuration	Structural weight (kg)	l_c	l_p	t_f	t_c	θ	t_p	t_{fc}	t_{fb}	t_{p1}	t_{p2}
S-1	Empty	1.26	20	5	1	0.5	63°	–	–	–	–	–
S-2	Single PML-A	1.37	20	5	1	0.5	63°	2	0.5	0.5	–	–
S-3	Single PML-A	1.48	20	5	1	0.5	63°	4	0.5	0.5	–	–
S-4	Single PML-A	1.59	20	5	1	0.5	63°	6	0.5	0.5	–	–
S-5	Single PML-B	1.59	20	5	1	0.5	63°	6	–	–	–	–
S-6	Double PMLs-A	1.59	20	5	1	0.5	63°	–	0.5	0.5	3	3

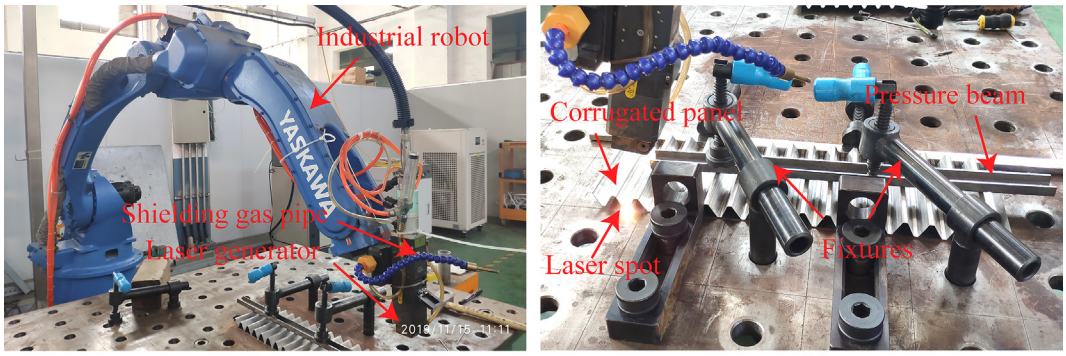

Fig. 2. (a) Fabrication setup of laser welding and (b) detailed fixture of laser welding process.

Table 2
Laser welding parameters employed in this study for welding steel plates having different thicknesses.

Welding condition	0.5 mm – 0.5 mm	0.5 mm – 1.0 mm	1.0 mm – 0.5 mm
Power (W)	1500	1700	1700
Welding speed (m/min)	3	4	2
Shielding gas flow (L/min)	15	15	15
Focal point position (mm)	0	0	0
Welding joint width (mm)	0.753	0.643	0.503

two weeks. Finally, LASCOR sandwich panels with either single or double PML-B face sheets were obtained after removing the mold, as shown in Fig. 4b and Fig. 4d. Meanwhile, the panel with single PML-A face sheet was fabricated, as shown in Fig. 4c. Notably, it was seen from Fig. 4 that the polyurea layers were well bonded with the base metal plates due to the excellent adhesiveness of polyurea. The thickness of each polyurea layer could be ensured with a constant weight and mass density.

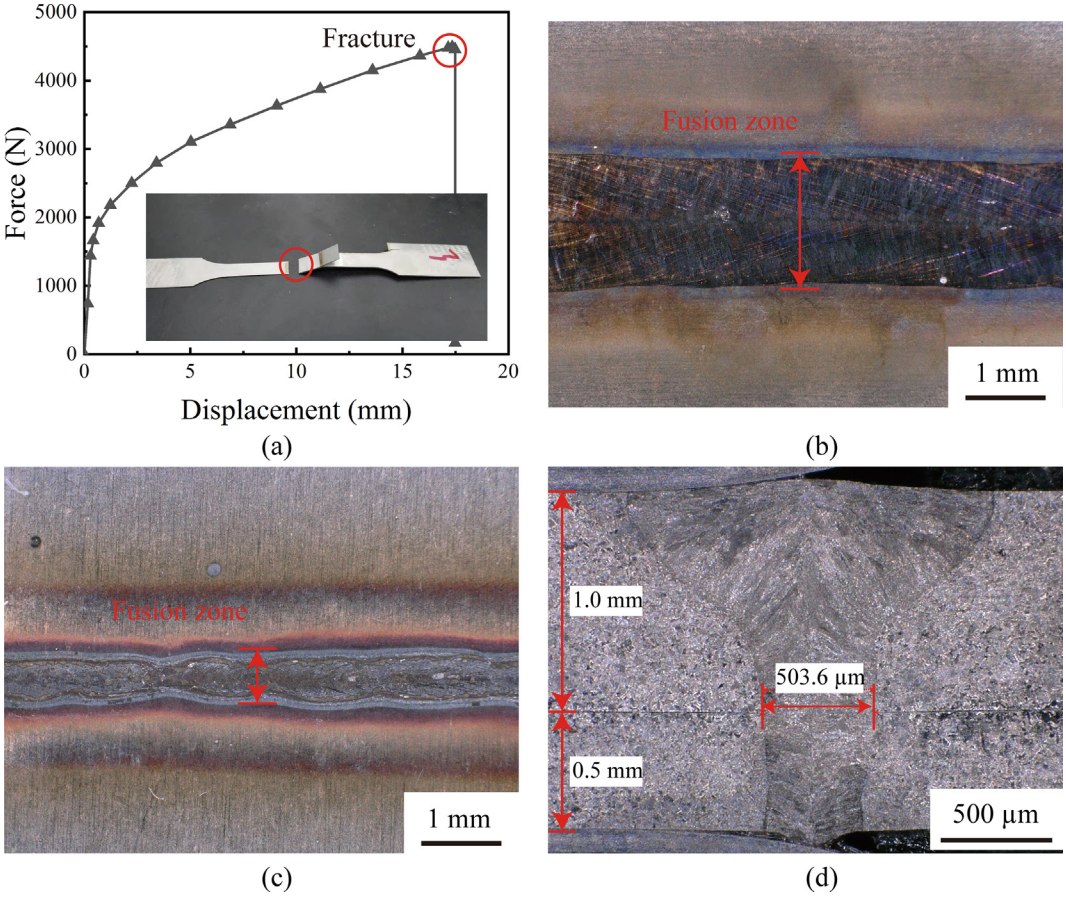

Fig. 3. (a) Standard tensile-shear testing curve of 1.0 mm–0.5 mm laser-welded lap joint. Corresponding optical microscope photography: (b) front side, (c) back side, and (d) cross section.

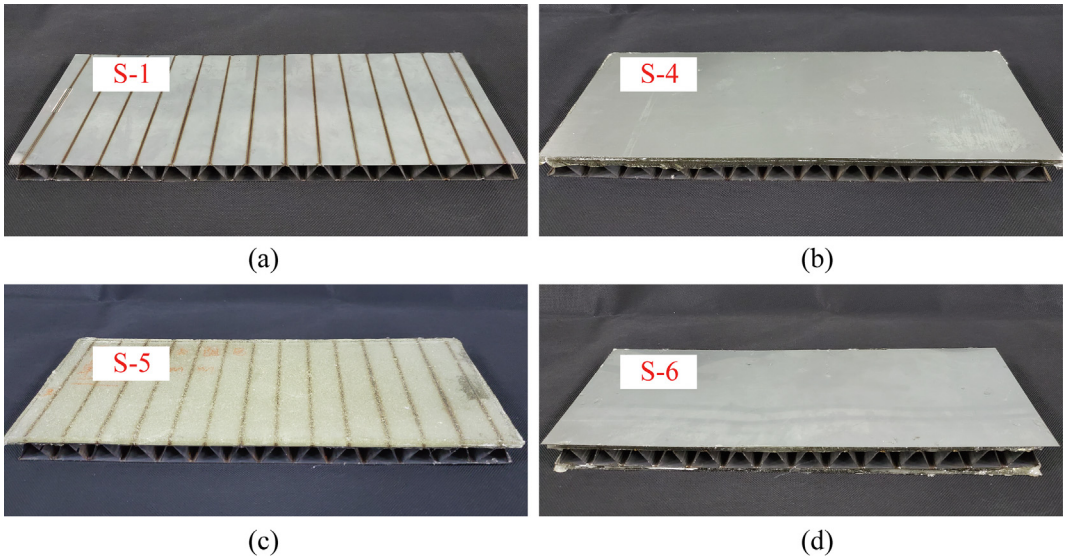

Fig. 4. As-fabricated corrugated sandwich panel (a) S-1 (without polyurea coating), (b) S-4 (with single PML-A face sheet), (c) S-5 (with single PML-B face sheet), and (d) S-6 (with double PML-A face sheets).

2.2. Material characterization

2.2.1. Quasi-static tensile test of the polyurea

To determine the mechanical properties of polyurea material, quasi-static uniaxial tensile tests were conducted at a strain rate $\dot{\varepsilon} = 2.0 \times 10^{-3} s^{-1}$ on a servo hydraulic test machine (Instron 5943, USA), as shown in Fig. 5a. Following previous studies of soft materials [28], standard tensile samples were cut from as-fabricated polyurea layers, and five nominally identical specimens were tested to ensure data accuracy. Force and displacement data generated in the test

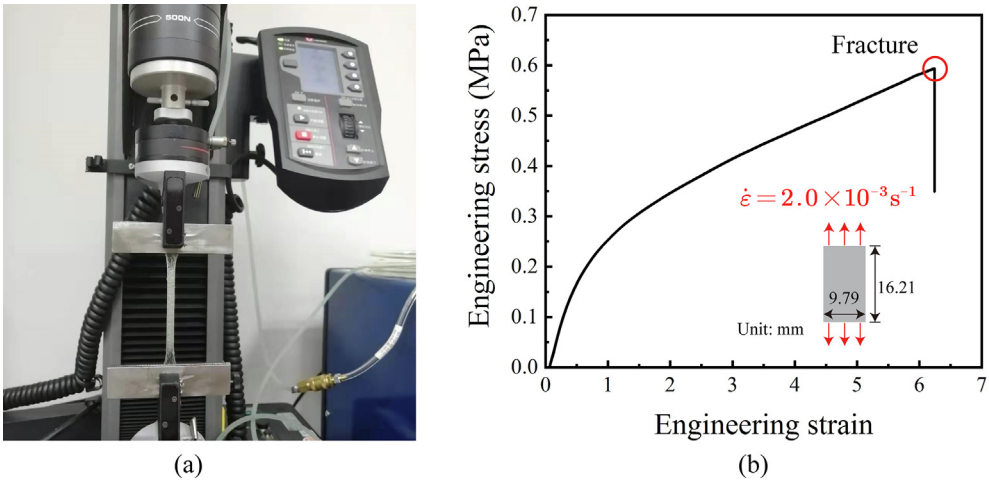

Fig. 5. (a) Quasi-static uniaxial tensile testing of as-prepared polyurea sample and (b) tensile engineering stress versus engineering strain curve of polyurea.

machine were simultaneously recorded, as shown in Fig. 5b in the format of average engineering stress versus engineering strain. The as-prepared polyurea firstly deformed linear elastically, then nonlinearly approached its initial yield stress, and further experienced continuous strain hardening deformation till fracture. Similar deformation trend was observed in other types of polyurea material [23]. Upon fitting the elastic portion of the deformation in Fig. 5b, the elastic modulus (Young's modulus) of the present polyurea was obtained as 0.562 MPa.

2.2.2. Dynamic thermomechanical analysis (DMA) of the polyurea

The Young's modulus E_p of polyurea should be represented by a complex quantity, revealing the dependence of its stiffness and damping properties on temperature and frequency. The real part of the complex term (storage modulus), E'_p, related to the elastic behavior of polyurea, while the imaginary component (loss modulus), E''_p, defined the energy dissipative ability of the material. Thus, the complex Young's modulus E_p could be expressed as:

$$E_p = E'_p + iE''_p = E'_p(1 + i\eta_p) \tag{2}$$

$$\eta_p = \frac{E''_p}{E'_p} \tag{3}$$

where η_p presents the damping loss factor of polyurea. To measure the storage modulus E'_p and damping loss factor η_p, dynamic thermomechanical analysis (DMA-Q800, TA) with tensile measurement mode was carried out. Note that, the DMA testing data of the as-fabricated polyurea was provided by Qingdao Shamu Advanced Material Co., Ltd. The results shown in Fig. 6 exhibited the sensitivity of both E'_p and η_p to temperature (−80–100 °C) and frequency (1, 10, 50, 100, 150 Hz). The storage modulus was positively related with testing frequency but negatively with temperature rise (Fig. 6a). As to the damping loss factor (Fig. 6b), at a fixed testing frequency, it firstly increased slightly with temperature rise (−80–40 °C), then quickly reached a plateau (−40–20 °C), and finally climbed to its peak (0.42–0.55) around a glass transition temperature (50–80 °C). On the other hand, increasing the excitation frequency led to higher glass transition temperature and larger damping loss factor.

2.2.3. Quasi-static tensile test of the 304 stainless steel

Uniaxial tensile test at a nominal strain rate of $\dot{\varepsilon} = 3.3 \times 10^{-3} s^{-1}$ was also conducted to determine the mechanical properties of 304 stainless steel (density $\rho_s = 7930\ kg/m^3$). According to recommendations of ISO standard 6892–1:2009, five standard dog-bone specimens were tested for accuracy. The average true stress versus true strain curve thus measured was presented in Fig. 7. Generally speaking, the 304 stainless steel may be regarded as an elastic, linearly hardening material, with Young's modulus $E_s = 200$ GPa and tangent modulus $E_t = 2$ GPa.

2.3. Modal vibration tests

Modal vibration tests were performed on as-fabricated sandwich samples (Table 1) as shown in Fig. 8. Each test sample was suspended on a metallic bracket with two elastic rubber ropes to simulate the free boundary condition. The experimental system was comprised of an impact hammer (PCB-086C03), an accelerometer (PCB-333B32), a dynamic signal analyzer, and a monitoring laptop loaded with a modal analysis software (DongHua Modal Analysis). With the method of point-by-point excitation adopted, the test samples were all divided into 28 regions linked by 45 points (marked in each sample). Once the accelerometer was placed on point 11, an impact force was applied by the impact hammer on points 1–45 in sequence. For consistence, the impact force was preset in the range of 40–50 N. To improve signal quality, the gauge and impact points were placed on the metallic plates instead of the soft polyurea layers, especially for specimen S-5. Signals from the accelerometer (response signal) and the impact hammer (force signal) were both transferred to the dynamic signal analyzer and then processed using the modal analysis software. Therefore, critical experimental results, including frequency/time response curves, natural frequencies, mode shapes and damping loss factors could be determined. For completeness, theoretical basis of the present experimental tests was briefly described below.

For a continuous system excited by a step input force vector $\{F(t)\}$, the governing differential equation could be expressed as:

$$[M]\{\ddot{x}\} + [C]\{\dot{x}\} + [K]\{x\} = \{F(t)\} \tag{4}$$

where $[M]$, $[C]$ and $[K]$ are the mass, damping and stiffness matrices of the system, respectively. The frequency response function (FRF) of the system could be obtained as:

$$H(j\omega) = \frac{X(j\omega)}{F(j\omega)} = \frac{1}{-\omega^2[M] + j\omega[C] + [K]} \tag{5}$$

where $F(j\omega)$ is the impulse input force imparted to the system using an impact hammer, $X(j\omega)$ represents the response of the system which is measured by the acceleration. Once the frequency response curve of Eq. (5) is determined, the resonant peak corresponding to the natural frequency $\omega^{(r)}$ could be acquired. Here, the superscript (r) signifies the r^{th} mode or the resonant peak. Near the resonant peak, two half-power points with $\sqrt{2}/2$ of the peak value are obtained, and the corre-

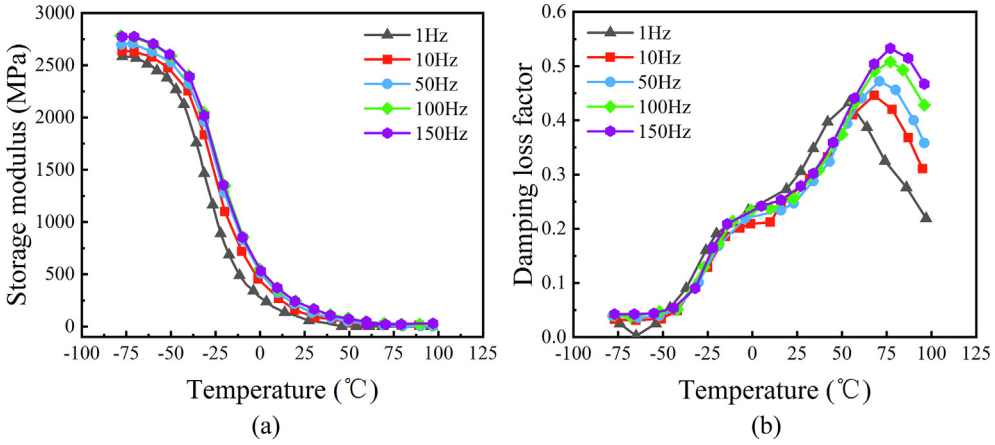

Fig. 6. DMA testing results of polyurea: (a) storage modulus and (b) damping loss factor.

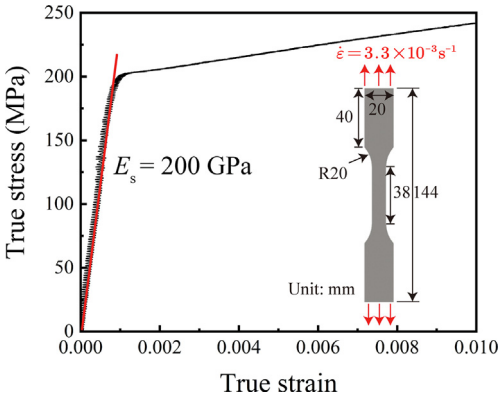

Fig. 7. Measured tensile true stress versus true strain curve of 304 stainless steel.

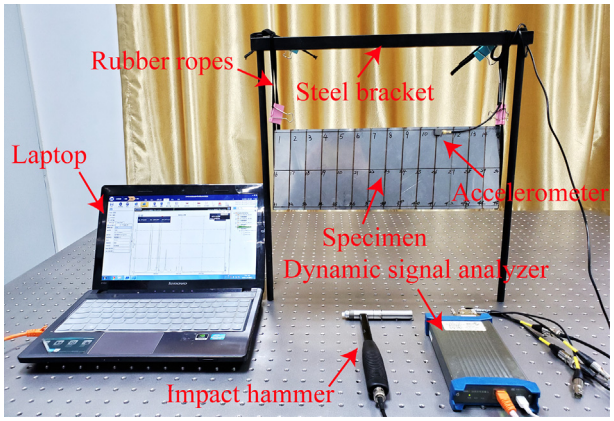

Fig. 8. Experimental setup of modal vibration test on as-fabricated sandwich panel.

sponding frequencies $\omega_a^{(r)}$ and $\omega_b^{(r)}$ could be employed to calculate the damping loss factor, as [29]:

$$\eta^{(r)} = \frac{2\left(\omega_b^{(r)} - \omega_a^{(r)}\right)}{\omega^{(r)}}, \omega_b^{(r)} > \omega_a^{(r)} \quad (6)$$

In the present modal vibration tests, the first three modes were investigated. For accuracy, the average data of three parallel tests were reported. More details of the experimental method were reported in a previous study [6].

3. Numerical prediction

Based on the commercially available finite element (FE) code ABAQUS/CAE 2016, a combined finite element-modal strain energy (FE-MSE) method was adopted to predict the vibration and damping properties of LASCOR sandwich panels with PML face sheets. Specifically, the modal characteristics (*e.g.,* natural frequencies, mode shapes, modal strain energy) of the undamped panels were firstly calculated using the traditional FE method, and then imported to obtain the damping loss factors of the damped panels by means of the MSE method [30]. The FE-MSE method was previously adopted to estimate the vibration and damping behaviors of fiber-reinforced composite lattice-core sandwich panels [31].

3.1. Finite element simulation

For FE simulation, both the face sheets and the corrugated core were modeled using 4-node doubly curved thin/thick shell elements S4R, while the polyurea layers were meshed using 8-node linear brick solid elements C3D8R. Based on tie constraint algorithm, all the components of the sandwich panel were perfectly bonded together. The so-called frequency analysis step with Lanczos eigensolver was conducted to obtain the first three modal characteristics, such as the natural frequencies and mode shapes. In this step, both the parent metal (304 stainless steel) and the polyurea material were considered as linear elastic materials, with the input parameters of the former obtained from Fig. 7. As to the viscoelastic polyurea, the real part of its complex Young's modulus (storage modulus), E'_p, should be employed in the FE model [30]. However, E'_p exhibited frequency dependency in the testing range, as shown in Fig. 6a. Thus, to improve the prediction accuracy, the frequency sensitivity of polyurea was taken into consideration in the current study. Similar to the previous literature [32], the detailed calculation principle was summarized in Fig. 9. Note that, the frequency corresponding to the initial storage modulus E'_{p0} was set as 1 Hz.

Limited by the frequency range of the present DMA tests (Fig. 6), storage modulus and damping loss factors within 0 ~ 150 Hz were obtained. However, the concerned first three natural frequencies might be above 150 Hz. Thus, in order to expand the frequency range to 150–1200 Hz, the Havriliak-Negami model [33,34] and the Kelvin-Voigt model [35] were introduced to fit the DMA testing data, respectively. This approach was also adopted by a recent study [36] for the same purpose. The two classical theoretical models could be expressed as:

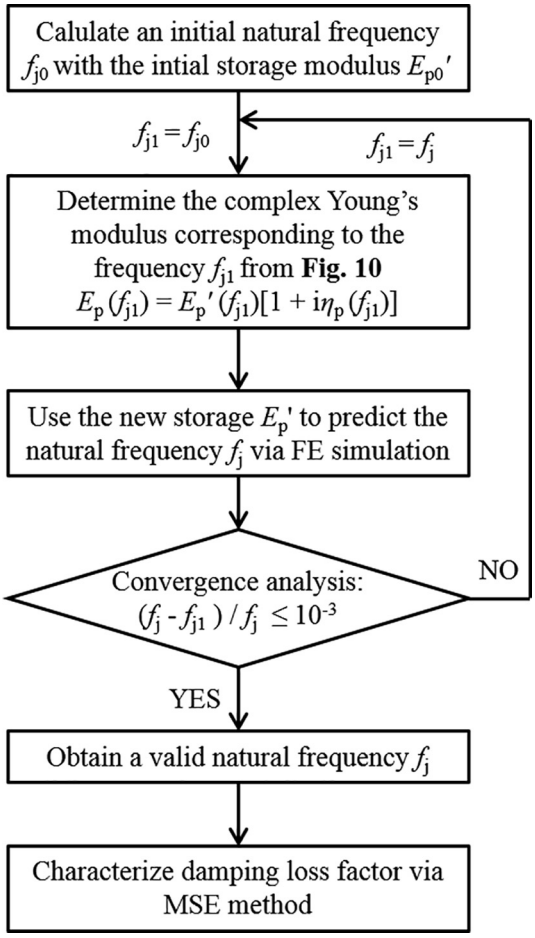

Fig. 9. The calculation procedure of FE-MSE method.

$$E_p'(f)=c_2+\frac{(c_1-c_2)\cos\left(c_4\tan^{-1}\left(\frac{(2\pi f)^{c_3}\sin\left(\frac{c_3\pi}{2}\right)}{1+(2\pi f)^{c_3}\cos\left(\frac{c_3\pi}{2}\right)}\right)\right)}{\left(1+2(2\pi f)^{c_3}\cos\left(\frac{c_3\pi}{2}\right)+(2\pi f)^{2c_3}\right)^{\frac{c_4}{2}}} \tag{7}$$

$$\eta_p(f)=\frac{d_1(2\pi f)^{d_3}\sin\left(\frac{d_3\pi}{2}\right)}{d_1(2\pi f)^{d_3}\cos\left(\frac{d_3\pi}{2}\right)+d_2} \tag{8}$$

where f is the testing frequency, c_1~c_4 are the undetermined coefficients of the Havriliak-Negami model, d_1~d_3 and are the undetermined coefficients of the Kelvin-Voigt model. As the present modal vibration tests were carried out at room temperature (25 °C), the DMA testing data of polyurea (Fig. 6) could be used to fit the above two theoretical models. Fig. 10 displayed the extended curves of storage modulus and damping loss factor. Both the storage modulus and damping loss factor soared in the low frequency range, but the increase slowed down with the increase of testing frequency. This trend of polyurea was similar to that reported for alternative viscoelastic materials [37].

3.2. Modal strain energy method

In addition to FE simulations detailed in the previous section, the damping loss factor of the proposed sandwich structure was further estimated by means of the modal strain energy (MSE) method introduced by Johnson and Kienholz [30]. Compared with directly solving the complex eigenvalues and eigenvectors of Eq. (4), the MSE method only needs to calculate the undamped modes; corresponding energy distributions can be obtained to determine the damping characteristics. The basic assumption of the MSE method is that the damped and undamped mode shapes of a structure are identical [30], so that the damping loss factor corresponding to the rth mode can be estimated as:

$$\eta^{(r)}=\frac{\Delta U^{(r)}}{U^{(r)}}=\frac{\sum_{i=1}^{m}\eta_s^{(r)}u_{s,i}^{(r)}+\sum_{j=1}^{n}\eta_p^{(r)}u_{p,j}^{(r)}}{\sum_{i=1}^{m}u_{s,i}^{(r)}+\sum_{j=1}^{n}u_{p,j}^{(r)}} \tag{9}$$

where the superscript (r) represents the rth mode, $\Delta U^{(r)}$, $U^{(r)}$ are the total stored strain energy and dissipated strain energy, respectively. $u_{s,i}^{(r)}$ is the stored energy of element i in the metallic sandwich component, $u_{p,j}^{(r)}$ is the stored energy of element j in the polyurea layer, while $\eta_s^{(r)}$ and $\eta_p^{(r)}$ are the material loss factors of 304 stainless steel and polyurea material corresponding to the rth natural frequency. Further, $u_{s,i}^{(r)}$ and $u_{p,j}^{(r)}$ can be written as:

$$u_{s,i}^{(r)}=\frac{1}{2}\sum\int_{V_{s,i}}\sigma_{kl}\varepsilon_{kl}dV_{s,i}(k,\ l=x,\ y,\ z) \tag{10}$$

$$u_{p,j}^{(r)}=\frac{1}{2}\sum\int_{V_{s,i}}\sigma_{kl}\varepsilon_{kl}dV_{p,j}(k,\ l=x,\ y,\ z) \tag{11}$$

where σ_{kl} and ε_{kl} $(k,\ l=x,\ y,\ z)$ are the stress and strain component, respectively. $V_{s,i}$ and $V_{p,j}$ are separately the volume of element i in the metallic sandwich component and the volume of element j in the polyurea layer. The global coordinate system $(x,\ y,\ z)$ attributes to the finite element model, as shown later in Fig. 14. In the current study, the damping loss factor of 304 stainless steel was set as 0.006 since it is insensitive to frequency according to existing studies [38]. By contrast, the damping loss factor of polyurea (Fig. 10b) was about two orders of magnitude higher. Eq. (9) indicated that the strain energy contribution of polyurea plays a vital role in the damping performance of the present sandwich panels having PML face sheets.

3.3. Mesh convergence

To determine the optimal mesh size for FE simulations, a mesh convergence study was carried out to ensure mesh refinement using different mesh sizes (1.5, 2, 3, 4, 5 mm). To this end, the first three natural frequencies of the undamped sandwich panel (i.e., without polyurea coating) were calculated via the above simulation process, as displayed in Fig. 11. The first three natural frequencies seemed to converge as the mesh size was reduced, and the difference in simulation results obtained with mesh sizes of 1.5 and 2 mm was not obvious. Thus, for balanced computational cost and numerical accuracy, the overall mesh size of 2 mm was adopted in all subsequent numerical simulations.

4. Results and discussion

4.1. Experimental results

Experimental results in terms of frequency/time response curves, natural frequencies, mode shapes and damping loss factors were presented in sequence for the sandwich panels of Table 1.

4.1.1. Frequency/time response curves

Firstly, the sample frequency response curves of panel S-1 (without polyurea coating) and panel S-2 (with single PML-A face sheet) were presented in Fig. 12a,b. The first three resonant peaks of S-1 were seen to be significantly higher and sharper compared to those of S-2. The difference in the shapes of resonant peaks was actually related to the characteristics of structural damping, as reasoned in a previous study [29]. To be specific, the results of Fig. 12a,b suggested that the damping performance of S-2 was much better than that of S-1. Further, Fig. 12c displayed the time response curves of these two specimens.

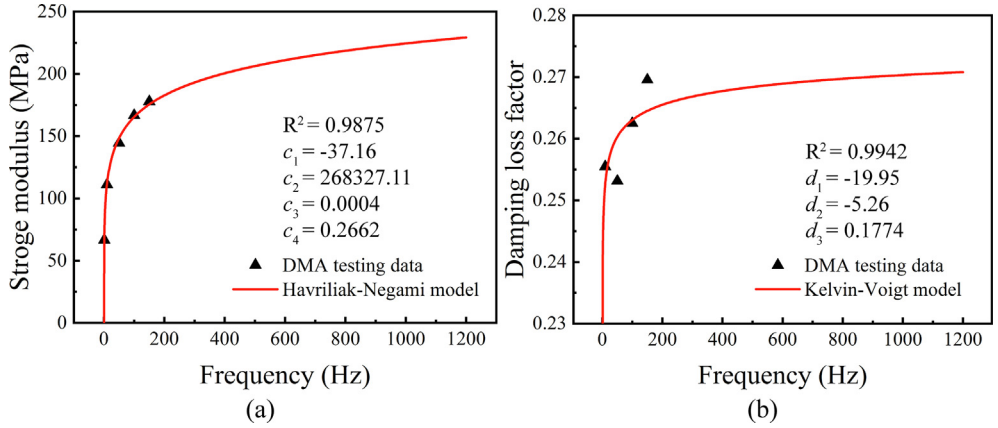

Fig. 10. Fitting curves of (a) storage modulus and (b) damping loss factor of polyurea as functions of testing frequency (0–1200 Hz) at room temperature.

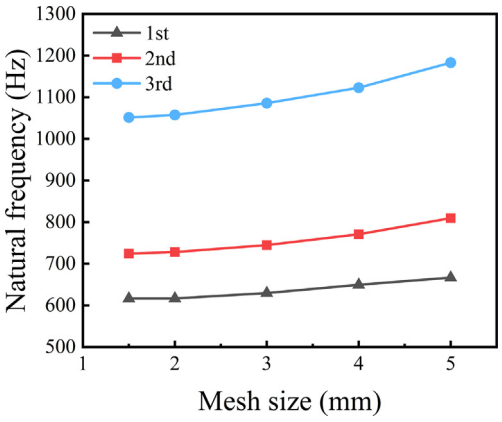

Fig. 11. Dependence on mesh size of the first three natural frequencies of sandwich panel without polyurea coating.

To facilitate visual comparison, the acceleration signals were normalized by their maximum acceleration values. The acceleration signal of S-1 decreased slowly and started to remain stable at 200 ms, while that of S-2 plummeted to zero within 80 ms. Evidently, excellent vibration attenuation was achieved in panel S-2. These results demonstrated that replacing the metal face sheets with PML face sheets indeed led to significantly enhance passive vibration suppression capability of corrugated sandwich panels.

4.1.2. Natural frequencies and mode shapes

Next, the effects of PML face sheets on the measured first three natural frequencies of as-fabricated sandwich panels were analyzed, as shown in Fig. 13a. Overall, the natural frequency range of the panels tested was within 1000 Hz. The natural frequencies of panel S-1 without polyurea coating were a little bit higher than those of the other five panels having PML face sheets, which was attributed to variations in flexural stiffness and structural weight [39]. With the same structural weight, the testing results of panels S-4, S-5 and S-6 were compared to estimate the influence of varying PML configurations. Among these three panels, the panel with a single PML-A face sheet (S-4) exhibited the highest natural frequencies, owing to its biggest flexural stiffness. With the same configuration (single PML-A face sheet), the results of S-2, S-3 and S-4 were further compared to evaluate the thickness effect of polyurea layer: the natural frequencies of sandwich panels with single PML-A face sheet increased with increasing polyurea layer thickness. The experimentally measured first mode shapes of panel S-4 were plotted in Fig. 14a. The first and third mode shapes of S-4 were both transverse bending shapes while the second mode shape was torsional shape. No longitudinal bending mode was observed from S-4, indicating that its flexural stiffness along the longitudinal direction was higher than that along the transverse direction. The remaining samples tested in this study exhibited the same first three mode shapes, so the results were not presented for brevity.

4.1.3. Damping loss factors

The dependence of damping loss factor on face sheet configuration was also analyzed, as shown in Fig. 13b. Sandwich panels with PML face sheets all exhibited damping loss factors more than 10 times larger relative to those of the undamped panel, demonstrating that the viscoelastic deformation of the embedded polyurea layers dissipated effectively the vibration energy. However, the damping loss factors of S-4 were significantly higher than those of S-5, revealing that PML-A face sheets (CLD treatment) led to a much higher level of structural vibration suppression than PML-B face sheets (FLD treatment). Since the first three modes were either bending or torsional modes, the constrained polyurea layer could dissipate a larger amount of vibration energy via transverse shear deformation. In contrast, the free polyurea layer dissipated the energy mainly via tensile/compressive deformation. Similar mechanisms were identified in a previous study [12]. As can be seen from Fig. 13b, increasing the polyurea layer thickness enabled the damping loss factors to improve effectively. This, however, would also increase sandwich weight and hence lead to an inevitable problem about damping loss efficiency, i.e., the ratio of damping loss factor and structural weight. Further, the top and bottom face sheets of sample S-6 both had PML-A laminate configurations, with each polyurea layer having a thickness of 3 mm. Compared to sample S-4 with a single constrained 6 mm polyurea layer, S-6 displayed a more desirable enhancement of damping to some extent. Consequently, varying and optimizing the distribution of polyurea layer on both face sheets could lead to more dissipation of passive vibration energy, and would be explored in subsequent FE simulations.

4.2. Validation and analysis

The first three natural frequencies, damping loss factors, and mode shapes were numerically calculated for samples S-1 to S-6 and compared with measurement results. Detailed comparisons of natural frequencies and damping loss factor were summarized in Table 3. Fig. 14 presented further the measured and predicted first three mode shapes of sample S-4. Overall, the current simulations provided a reasonable prediction on the vibration and damping characteristics of LASCOR sandwich panels with PML face sheets. However, some discrepancies did exist, especially in the third natural frequency (Table 3). According to our previous analysis [6], the natural frequencies were sensitive to

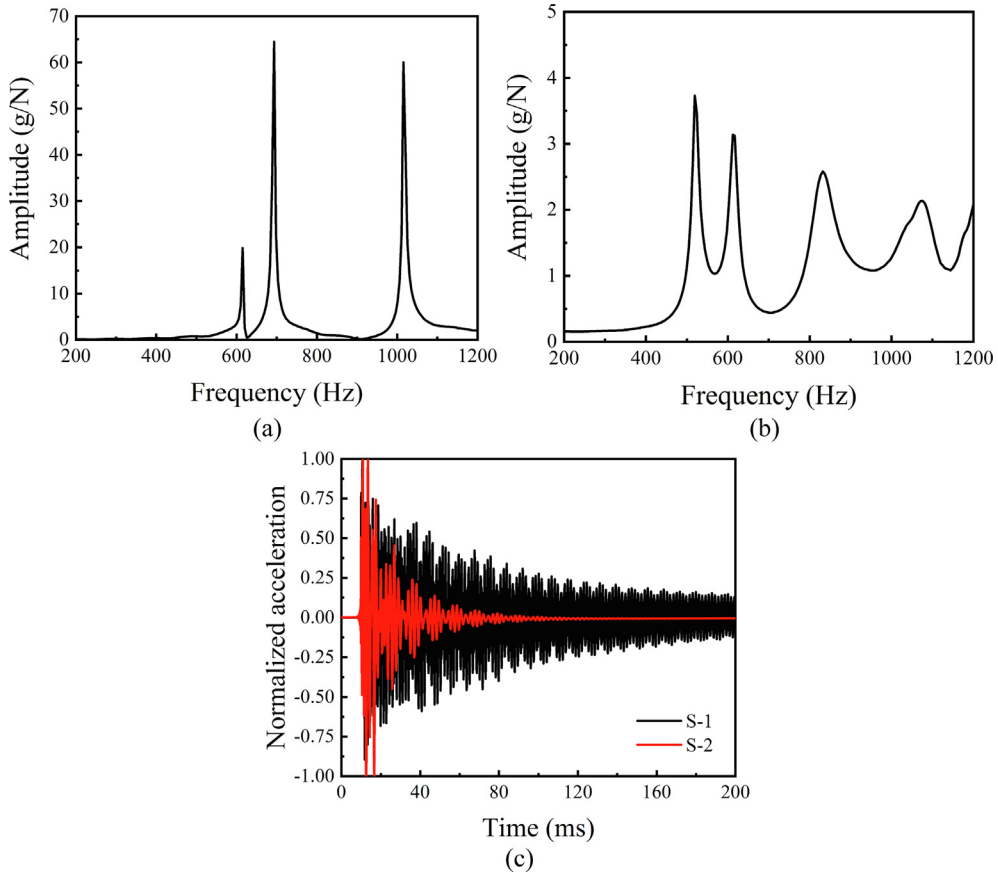

Fig. 12. Measured frequency response curves of (a) S-1 (without polyurea coating) and (c) S-2 (with single PML-A face sheet), and (c) their corresponding time response curves.

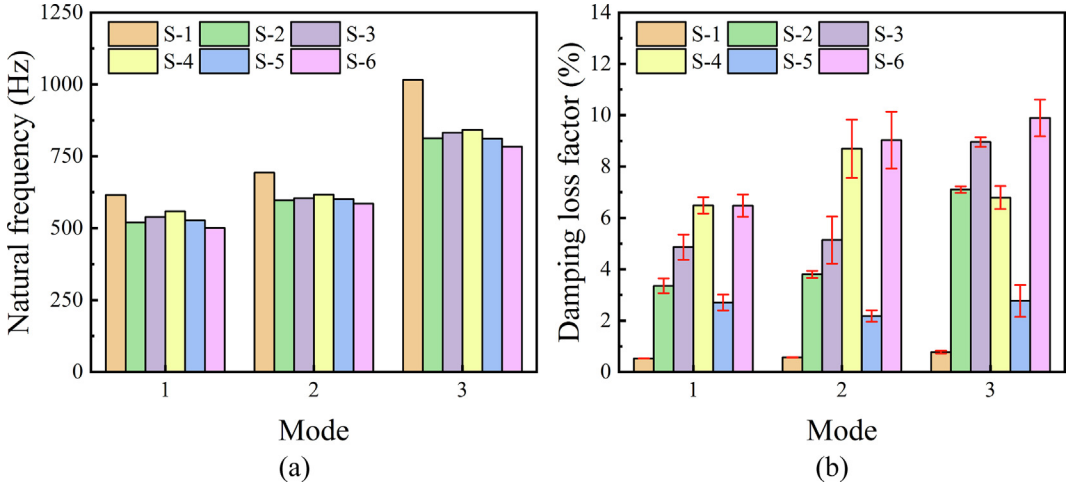

Fig. 13. Measured first three (a) natural frequencies and (b) damping loss factors of corrugated sandwich panels with and without PML face sheets.

the boundary condition, the laser welding defects, the corrugation forming defects, and so on. On the other hand, the structural damping characteristics were associated with the fabrication process, the boundary condition, and the testing set-up [17,40]. For instance, the rubber ropes might cause an extra damping effect but this effect was ignored in the current simulation. In addition, the fabrication defects of laser welding joints and polyurea layers were not taken into account. Nonetheless, although it was quite difficult to eliminate the above-mentioned error sources completely, the present numerical simulations were accurate enough and could be exploited to provide further analysis of the physical mechanisms underlying damping enhancement.

4.3. Discussion

Thus far, it had been demonstrated, both experimentally and numerically, that the strategy of replacing monolithic metallic face sheets by PML laminates could significantly enhance the vibration

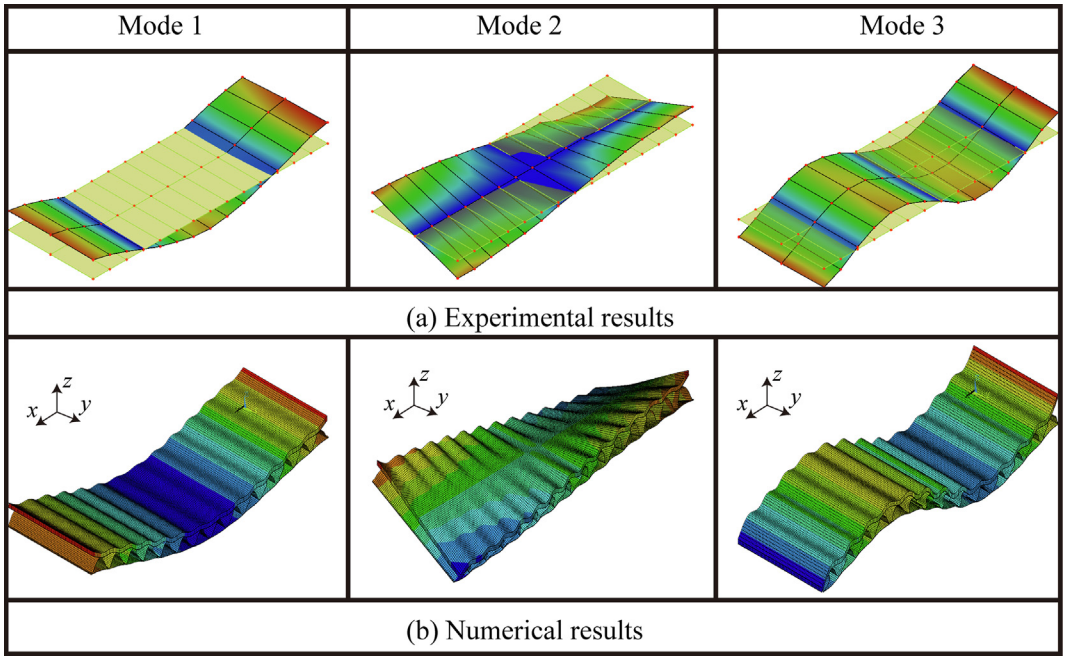

Fig. 14. First three mode shapes of specimen S-4 obtained from (a) experimental tests and (b) FE simulations.

Table 3
Comparative analysis of experimental measurements and FE simulations.

Specimen	Natural frequency (Hz)			Damping loss factor (%)		
	1st	2nd	3rd	1st	2nd	3rd
S-1	615.2 (616.75)	693.4 (728.13)	1015.6 (1057.6)	0.527 ± 0.003 (0.600)	0.575 ± 0.004 (0.600)	0.776 ± 0.029 (0.600)
S-2	519.5 (577.32)	597.5 (665.29)	812.4 (969.08)	3.355 ± 0.287 (4.593)	3.800 ± 0.139 (5.455)	7.104 ± 0.128 (6.735)
S-3	539.0 (590.24)	604.6 (677.55)	832.0 (1001.50)	4.865 ± 0.490 (5.328)	5.137 ± 0.917 (6.763)	8.956 ± 0.185 (7.923)
S-4	558.5 (597.08)	617.0 (680.65)	841.7 (1014.80)	6.487 ± 0.320 (5.991)	8.694 ± 1.137 (7.773)	6.792 ± 0.446 (8.859)
S-5	526.6 (565.84)	601.3 (676.07)	811.8 (1000.50)	2.703 ± 0.313 (1.966)	2.180 ± 0.220 (2.494)	2.773 ± 0.622 (3.016)
S-6	500.4 (559.24)	585.9 (629.75)	783.6 (935.02)	6.480 ± 0.438 (8.155)	9.028 ± 1.108 (10.101)	9.890 ± 0.712 (11.920)

*Numbers in parentheses are numerically predicted results.

damping characteristics of LASCOR sandwich panels under edge-free boundary condition. Constrained layer treatment (PML-A laminate) was found to be far more effective than free layer treatment (PML-B laminate) in damping enhancement. For the cases considered in the present study, the existence of polyurea layer increased the whole mass of the sandwich by a maximum of 26.2%, but the enhancement of the first three damping loss factors was more than 10 times relative to the control sandwich without polyurea coating, with a slight decline in natural frequencies. Note that the samples prepared for the present modal vibration tests were not optimally designed. In view of the measurement results, two critical issues were worthy of further discussion, namely, polyurea layer thickness and distribution of polyurea layers.

4.3.1. Effect of polyurea layer thickness

Firstly, the influence of polyurea layer thickness on vibration damping of sandwich panels with single PML-A face sheets was discussed. The numerical results shown in Fig. 15a,b exhibited a positive correlation between natural frequencies/damping loss factors and polyurea layer thickness, which could be explained as follows. Based on the first shear deformation theory, Timoshenko [39] proposed an analytical solution to the first natural frequency of prismatic beams with simple supported ends, as:

$$p_m = \frac{\pi^2}{L^2}\sqrt{\frac{EIg}{\rho\Omega}}\left[1 - \frac{1}{2}\frac{\pi^2 I}{L^2\Omega}\left(1 + \frac{E}{\lambda\Lambda}\right)\right] \tag{12}$$

where Λ is the modulus of transverse shear stiffness, λ is a constant relying upon the shape of beam cross section, $L$is the length of a wave, EI is the flexural stiffness of the prismatic bar, Ω is the area of the cross section, and ρ/g is the density of the base material. The flexural stiffness of a corrugated sandwich panel is mainly contributed by the face sheets, while its shear stiffness is induced by the corrugated core. Therefore, based on Eq. (12), it could be concluded that increasing the embedded polyurea layer thickness could improve the flexural stiffness of the panel and hence increase its natural frequencies. The damping loss factors exhibited a similar variation trend with polyurea layer thickness, as illustrated in Fig. 14b. Unlike the prior research [16], the damping loss factor of the torsional mode (the 2nd mode) lied in the middle of the first three modes. According to the theoretical basis of the MSE method, the damping loss factor was directly associated with the modal strain energy proportion of the constrained polyurea layer(s). That is, a larger amount of the stored strain energy in the sandwich panel should be dissipated via the viscoelastic deformation of the constrained polyurea layer(s). As shown in Fig. 15c, the modal strain energy proportion of the polyurea layer increased with its thickness and the mode order, which well explained the trend observed in the modal tests (Fig. 13b). To achieve a balance in damping and structural weight, the damping loss efficiency was introduced, as:

$$\text{Damping loss efficiency} = \frac{\text{Damping loss factor}}{\text{Structural weight}} \tag{13}$$

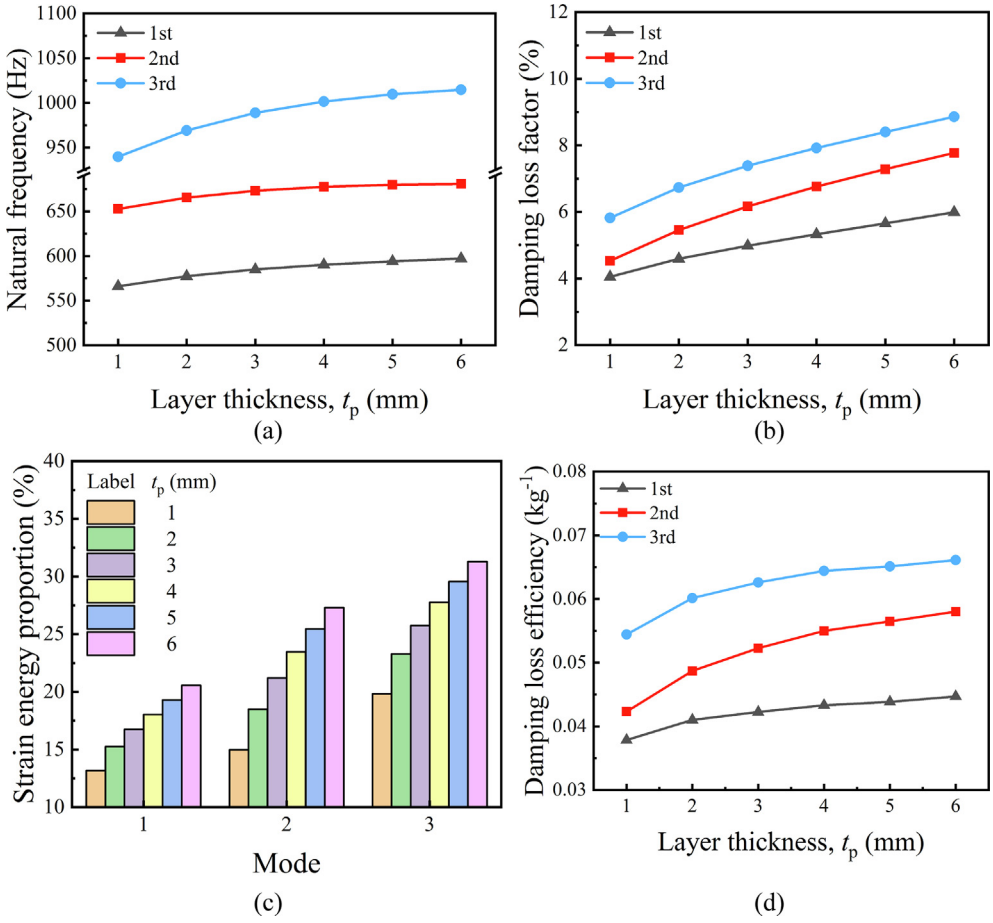

Fig. 15. Effect of polyurea layer thickness on (a) natural frequencies, (b) damping loss factors, (c) strain energy proportion and (d) damping loss efficiency for the first three vibration modes.

Fig. 15d plotted the numerically calculated damping loss efficiency as a function of polyurea layer thickness for the first three vibration modes, which was seen to increase rapidly with increasing layer thickness, eventually reaching a maximum as a certain layer thickness (about 6 mm in the current cases). The damping loss efficiency is valuable for engineers to design the most effective damping strategy with due consideration of structural weight.

4.3.2. Effect of polyurea layer distribution

Consider next the other possible design scenario, i.e., the distribution of constrained polyurea layers. According to the experimental results presented in Section 4.1, the LASCOR sandwich panel with double 3 mm constrained polyurea layers exhibited superior damping behavior to the panel with a single 6 mm constrained polyurea layer. Inspired by this, a dimensionless parameter called the thickness ratio t_{p1}/t_{p2} was introduced to quantify the sensitivity of vibration damping to thickness variations of polyurea layers, i.e, 1/5, 2/4, 3/3, 4/2, 5/1, with the total thickness fixed at 6 mm. Fig. 16a,b plotted the numerically predicted natural frequencies and damping loss factors as functions of t_{p1}/t_{p2}. Both the natural frequencies and damping loss factors peaked at the thickness ratio of 3/3. Meanwhile, the damping loss factors of panels with varying thickness ratios were compared with those of the panel with a single 6 mm constrained polyurea layer. As shown in Fig. 16c, the damping loss factor could be enhanced by as large as 28–36% at the thickness of 3/3. The enhancement mechanism of distributed polyurea layers was analyzed by calculating the modal strain energy proportion of each layer, and the results were displayed in Fig. 16d. Consistent with the results of Fig. 16a–c, the proportion of modal strain energy also peaked at the case of uniform polyurea distribution, i.e., the symmetric configuration of PML-A laminates outperformed the asymmetric configurations in so far as passive vibration damping is of concern.

5. Concluding remarks

The main motivation of this investigation was to propose novel LASCOR (laser-welded corrugated-core) sandwich panels with PML (polyurea-metal laminate) face sheets and further evaluate their vibration damping performance. A mixed experimental and numerical approach was employed to quantify the benefits of PML face sheets and explore the mechanisms underlying damping enhancement, with main conclusions summarized as below.

(i) Replacing monolithic face sheets by PML laminates enhanced significantly the damping loss factors of the sandwich panel with a slight decline in natural frequencies, due mainly to effective vibration energy dissipation of the constrained polyurea layers;
(ii) The mixed FE-MSE (finite element-modal strain energy) method with consideration of the frequency-dependent damping behaviors of polyurea was proposed, which provided reasonable predictions of natural frequencies, damping loss factors, and mode shapes;
(iii) The benefit of PML face sheets for enhanced vibration damping was correlated strongly with the polyurea layer thickness and the distribution of constrained polyurea layers.

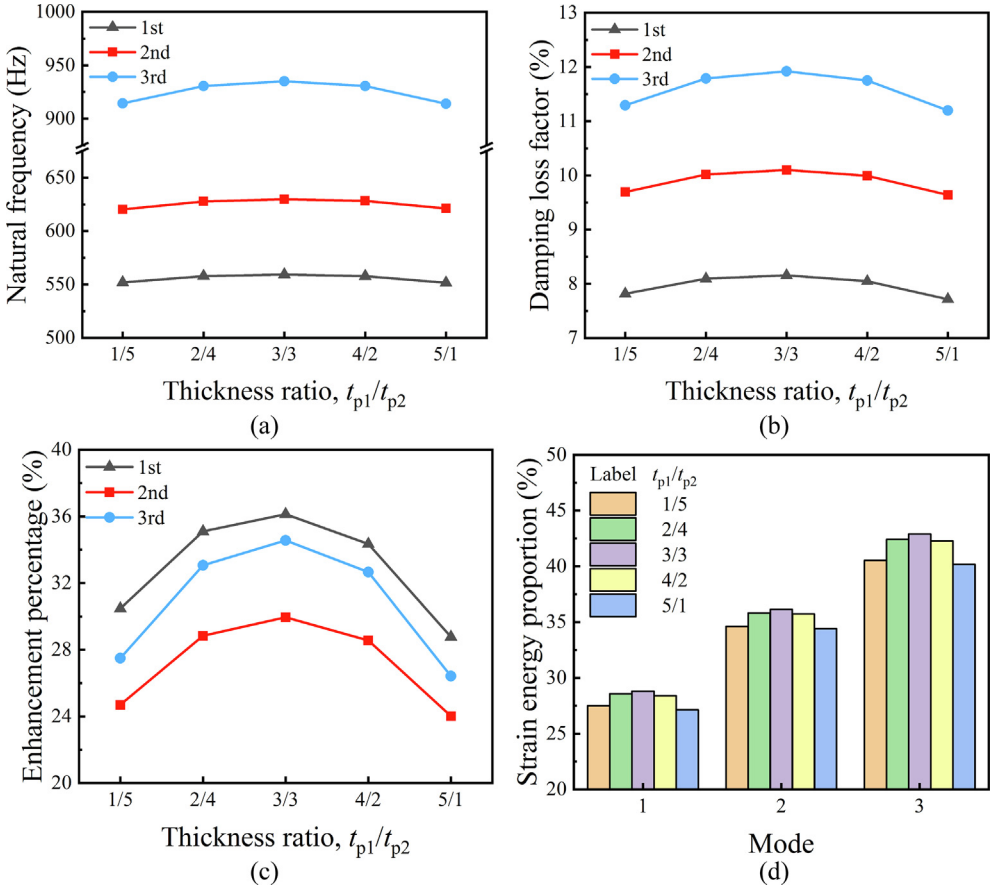

Fig. 16. Effect of polyurea layer distribution on (a) natural frequencies, (b) damping loss factors, (c) enhancement percentage and (d) strain energy proportion for the first three vibration modes.

This work provided an effective strategy for designing lightweight sandwich structures with superior vibration damping characteristics, and contributed further fundamental research for multifunctional engineering structures requiring simultaneous structural stiffness and passive vibration suppression, such as ship hulls, automotive bodies and pulse detonation engines.

Declaration of Competing Interest

The authors declare that they have no known competing financial interests or personal relationships that could have appeared to influence the work reported in this paper.

Acknowledgments

This work was supported by National Key Research and Development Program of China (2017YFB1102801), National Natural Science Foundation of China (11972185 and 11902148), Open Project for Key Laboratory of Intense Dynamic Loading and Effect (KLIDLE1801), Aviation Science Foundation Project (20170970002), Natural Science Fund Project in Jiangsu Province (BK20190392), and Open Fund of State Key Laboratory of Mechanics and Control of Mechanical Structures (MCMS-E0219K02 and MCMS-I-0219K01) and State Key Laboratory of Smart Manufacturing for Special Vehicles and Transmission System (GZ2019KF015). XW, XL and RPY are grateful to Donghua Testing Technology Co. Ltd. for the helpful technical assistance of modal vibration testing.

References

[1] Evans AG, Hutchinson JW, Fleck NA, Ashby MF, Wadley HNG. The topological design of multifunctional cellular metals. Prog Mater Sci 2001;46:309–27. https://doi.org/10.1016/S0079-6425(00)00016-5.

[2] Zhang Q, Yang X, Li P, Huang G, Feng S, Shen C, et al. Bioinspired engineering of honeycomb structure – Using nature to inspire human innovation. Prog Mater Sci 2015;74:332–400. https://doi.org/10.1016/j.pmatsci.2015.05.001.

[3] Côté F, Deshpande VS, Fleck NA, Evans AG. The out-of-plane compressive behavior of metallic honeycombs. Mater Sci Eng A 2004;380:272–80. https://doi.org/10.1016/j.msea.2004.03.051.

[4] Yan LL, Han B, Yu B, Chen CQ, Zhang QC, Lu TJ. Three-point bending of sandwich beams with aluminum foam-filled corrugated cores. Mater Des 2014;60:510–9. https://doi.org/10.1016/j.matdes.2014.04.014.

[5] Han B, Yu B, Xu Y, Chen CQ, Zhang QC, Lu TJ. Foam filling radically enhances transverse shear response of corrugated sandwich plates. Mater Des 2015;77:132–41. https://doi.org/10.1016/j.matdes.2015.03.050.

[6] Wang X, Zhao ZY, Li L, Zhang ZJ, Zhang QC, Han B, et al. Free vibration behavior of Ti-6Al-4V sandwich beams with corrugated channel cores: experiments and simulations. Thin-Walled Struct 2019;135:329–40. https://doi.org/10.1016/j.tws.2018.11.008.

[7] Lu TJ, Hess A, Ashby MF. Sound absorption in metallic foams. J Appl Phys 1999;85:7528–39. https://doi.org/10.1063/1.370550.

[8] Wang X, Yu RP, Zhang QC, Li L, Li X, Zhao ZY, et al. Dynamic response of clamped sandwich beams with fluid-fillied corrugated cores. Int J Impact Eng 2020;139:. https://doi.org/10.1016/j.ijimpeng.2020.103533103533.

[9] Yu R, Wang X, Zhang Q, Li L, He S, Han B, et al. Effects of sand filling on the dynamic response of corrugated core sandwich beams under foam projectile impact. Compos Part B 2020;197:. https://doi.org/10.1016/j.compositesb.2020.108135108135.

[10] Lakes RS. High damping composite materials. J Compos Mater 2008;36:287–97. https://doi.org/10.1106/002199802023538.

[11] Ashby MF. Materials selection in mechanical design. Fifth ed. Butterworth-Heinemann; 2017. https://doi.org/10.1007/978-3-319-05203-8_21.

[12] Kerwin Jr EM. Damping of flexural waves by a constrained viscoelastic layer. J Acoust Soc Am 1959;31:952–62.

[13] Oberst H, Frankenfeld K. Über die Dämpfung der Biegeschwingungen dünner Bleche durch fest haftende Beläge. Acta Acust United with Acust 1952;2:181–94.
[14] Kerwin Jr EM. Macromechanisms of damping in composite structures. In: Lazan BJ, editor. Intern. Frict. Damping, Cycl. Plast.. West Conshohocken, PA: ASTM International; 1965. p. 125–49. 10.1520/STP43767S.
[15] Ungar EE, Kerwin Jr EM. Plate damping due to thickness deformations in attached viscoelastic layers. J Acoust Soc Am 1964;36:386–92.
[16] Yang JS, Xiong J, Ma L, Wang B, Zhang GQ, Wu LZ. Vibration and damping characteristics of hybrid carbon fiber composite pyramidal truss sandwich panels with viscoelastic layers. Compos Struct 2013;106:570–80. https://doi.org/10.1016/j.compstruct.2013.07.015.
[17] Yang JS, Xiong J, Ma L, Zhang GQ, Wang XT, Wu LZ. Study on vibration damping of composite sandwich cylindrical shell with pyramidal truss-like cores. Compos Struct 2014;117:362–72. https://doi.org/10.1016/j.compstruct.2014.06.042.
[18] Yang JS, Xiong J, Ma L, Feng LN, Wang SY, Wu LZ. Modal response of all-composite corrugated sandwich cylindrical shells. Compos Sci Technol 2015;115:9–20. https://doi.org/10.1016/j.compscitech.2015.04.015.
[19] Chen YL, Wang XT, Ma L. Damping mechanisms of CFRP three-dimensional double-arrow-head auxetic metamaterials. Polym Test 2020;81:106189. https://doi.org/10.1016/j.polymertesting.2019.106189.
[20] Ma L, Chen YL, Yang JS, Wang XT, Ma GL, Schmidt R, et al. Modal characteristics and damping enhancement of carbon fiber composite auxetic double-arrow corrugated sandwich panels. Compos Struct 2018;203:539–50. https://doi.org/10.1016/j.compstruct.2018.07.006.
[21] Bai Y, Yu K, Zhao J, Zhao R. Experimental and simulation investigation of temperature effects on modal characteristics of composite honeycomb structure. Compos Struct 2018;201:816–27. https://doi.org/10.1016/j.compstruct.2018.06.106.
[22] Grujicic M, Pandurangan B, Bell WC, Cheeseman BA, Yen CF, Randow CL. Molecular-level simulations of shock generation and propagation in polyurea. Mater Sci Eng A 2011;528:3799–808. https://doi.org/10.1016/j.msea.2011.01.081.
[23] Raman SN, Ngo T, Lu J, Mendis P. Experimental investigation on the tensile behavior of polyurea at high strain rates. Mater Des 2013;50:124–9. https://doi.org/10.1016/j.matdes.2013.02.063.
[24] Huang W, Yang Y, Li H, Lyu P, Zhang R. Characterization and damping property of a modified polyurea material. DEStech Trans Mater Sci Eng 2017.
[25] Iqbal N, Tripathi M, Parthasarathy S, Kumar D, Roy PK. Polyurea coatings for enhanced blast-mitigation: a review. RSC Adv 2016;6:109706–17. https://doi.org/10.1039/c6ra23866a.
[26] Amini MR, Simon J, Nemat-Nasser S. Investigation of effect of polyurea on response of steel plates to impulsive loads in direct pressure-pulse experiments. Mech Mater 2010;42:615–27. https://doi.org/10.1016/j.mechmat.2009.09.009.
[27] Amini MR, Isaacs JB, Nemat-Nasser S. Experimental investigation of response of monolithic and bilayer plates to impulsive loads. Int J Impact Eng 2010;37:82–9. https://doi.org/10.1016/j.ijimpeng.2009.04.002.
[28] Sun JY, Zhao X, Illeperuma WRK, Chaudhuri O, Oh KH, Mooney DJ, et al. Highly stretchable and tough hydrogels. Nature 2012;489:133–6. https://doi.org/10.1038/nature11409.
[29] Chopra AK. Dynamics of structures: Theory and applications to earthquake engineering. Fifth. ed. Pearson; 2017.
[30] Johnson CD, Kienholzt DA. Finite element prediction of damping in structures with constrained viscoelastic layers. AIAA J 1982;20:1284–90.
[31] Yang JS, Ma L, Schmidt R, Qi G, Schröder KU, Xiong J, et al. Hybrid lightweight composite pyramidal truss sandwich panels with high damping and stiffness efficiency. Compos Struct 2016;148:85–96. https://doi.org/10.1016/j.compstruct.2016.03.056.
[32] Ghorbel A, Akrout A, Abdennadher M, Bouzouane B, Boukharouba T, Haddar M. Ultra-thin films inter-facial shear effects on modal damping characterization of laminated plate. Appl Acoust 2017;128:71–82. https://doi.org/10.1016/j.apacoust.2017.01.008.
[33] Havriliak S, Negami S. A complex plane analysis of α-dispersions in some polymer systems. J Polym Sci Part C Polym Symp 2007;14:99–117. https://doi.org/10.1002/polc.5070140111.
[34] Madigosky WM, Lee GF, Niemiec JM. A method for modeling polymer viscoelastic data and the temperature shift function. J Acoust Soc Am 2006;119:3760–5. https://doi.org/10.1121/1.2195292.
[35] Butcher EA, Segalman DJ. Characterizing damping and restitution in compliant impacts via modified k-v and higher-older linear viscoelastic models. J Appl Mech Trans ASME 2000;67:831–4. https://doi.org/10.1115/1.1308578.
[36] Liu Y, Liu Z, Song Q, Wang B. Analysis and implementation of chatter frequency dependent constrained layer damping tool holder for stability improvement in turning process. J Mater Process Technol 2019;266:687–95. https://doi.org/10.1016/j.jmatprotec.2018.11.033.
[37] Zhou XQ, Yu DY, Shao XY, Zhang SQ, Wang S. Research and applications of viscoelastic vibration damping materials: a review. Compos Struct 2016;136:460–80. https://doi.org/10.1016/j.compstruct.2015.10.014.
[38] Colakoglu M, Jerina KL. Damping behaviour of cyclically deformed 304 stainless steel. Indian J Eng Mater Sci 2003;10:480–5.
[39] Timoshenko SP. On the correction for shear of the differential equation for transverse vibrations of prismatic bars. Philos Mag 1921;41:744–6. https://doi.org/10.1080/14786442108636264.
[40] Chandra R, Singh SP, Gupta K. Damping studies in fiber-reinforced composites – a review. Compos Struct 1999;46:41–51. https://doi.org/10.1016/S0263-8223(99)00041-0.